Direct determination of the excited state energies of the xanthophylls diadinoxanthin and diatoxanthin from Phaeodactylum tricornutum

ARTICLE *in* CHEMICAL PHYSICS LETTERS · JUNE 2010

Impact Factor: 1.9 · DOI: 10.1016/j.cplett.2010.05.051

Chemical Physics Letters 493 (2010) 353–357

Contents lists available at ScienceDirect

Chemical Physics Letters

journal homepage: www.elsevier.com/locate/cplett

Direct determination of the excited state energies of the xanthophylls diadinoxanthin and diatoxanthin from *Phaeodactylum tricornutum*

Miriam M. Enriquez [a], Amy M. LaFountain [a], James Budarz [a], Marcel Fuciman [a], George N. Gibson [b], Harry A. Frank [a,*]

[a] Department of Chemistry, University of Connecticut, Storrs, CT 06269-3060, USA
[b] Department of Physics, University of Connecticut, Storrs, CT 06269-3046, USA

ARTICLE INFO

Article history:
Received 2 April 2010
In final form 17 May 2010
Available online 21 May 2010

ABSTRACT

Steady-state and femtosecond time-resolved transient absorption spectra of diadinoxanthin and diatoxanthin were measured in the visible and near-infrared (NIR) regions at 293 K. The difference in energy between the visible $S_0 \rightarrow S_2$ transitions from the steady-state absorption measurements and the $S_1 \rightarrow S_2$ transitions observed in the transient absorption spectra in the NIR region yields precise values of the S_1 energies. The data are important for evaluating the mechanism by which excess energy is dissipated by algal systems that interconvert these xanthophylls in response to changes in photon flux levels in the marine environment.

1. Introduction

Diadinoxanthin and diatoxanthin (Fig. 1) are xanthophylls that carry out light harvesting in marine phytoplankton [1–3]. They are also critical components in a defense mechanism that protects diatoms and dinoflagellates from photodamage due to excess light absorption [3,4]. Diadinoxanthin and diatoxanthin are enzymatically interconverted in algal systems such as *Phaeodactylum tricornutum* at a rate that depends on light flux levels [5,6]. Upon exposure to high irradiances, diadinoxanthin is de-epoxidized to form diatoxanthin, and this has been correlated with the quenching of chlorophyll (Chl) *a* fluorescence [7,8]. Upon return of the system to low light levels, diatoxanthin is re-epoxidized to diadinoxanthin. Chemical inhibition of the de-epoxidation of diadinoxanthin to diatoxanthin using dithiothreitol results in photo-induced damage to the photosynthetic apparatus because the excess excitation energy can no longer be dissipated [8].

The molecular details by which photoprotection is accomplished in green plants and algae are still unclear, but current debate has focused primarily on two mechanisms. The first is 'direct quenching' where the de-epoxidation of diadinoxanthin to diatoxanthin (or in green plants, of violaxanthin to zeaxanthin) generates a low-lying electronic state into which excess energy may flow and be dissipated harmlessly as heat. The low-lying state may be the S_1 state of a xanthophyll [9–11], or the process may involve the transfer of an electron between a xanthophyll and a Chl to facilitate quenching [12]. The second photoprotection mechanism is termed 'indirect quenching' whereby xanthophylls are thought to control the aggregation state of antenna complexes which then leads to quenching [13–15].

An important factor bearing on the question of whether xanthophylls can function as direct quenchers is the energy of their lowest-lying excited state, S_1. The fact that direct absorption from the ground state, S_0 ($1^1A_g^-$), to S_1 ($2^1A_g^-$) is forbidden by both symmetry and pseudo-parity selection rules [16–18] has rendered determinations of the precise S_1 energies of xanthophylls difficult. It is important to note that although xanthophylls do not strictly adhere to C_{2h} symmetry, but the molecules nevertheless exhibit many of the spectral characteristics of the parent polyenes to which these irreducible representations do apply. Indirect methods of determining S_1 energies have made use of correlations between fluorescence spectra and singlet state lifetimes [19–21] from shorter polyenes and carotenoids whose S_1 energies are more easily determined. Direct determinations of S_1 energies of carotenoids have been carried out using fluorescence [22–25], resonance Raman (rR) [26–28], and two-photon [29–31] spectroscopy, but each of these methods suffers from one or more shortcomings including low spectral resolution, interferences from fluorescing impurities, difficult sample preparation and handling, or systematic errors introduced by the technique probing different subsets of molecules in the sample.

In previous work [20], the S_1 energies of diadinoxanthin and diatoxanthin were determined indirectly to be 15 210 cm^{-1} and 14 620 cm^{-1}, respectively, by measuring the S_1 lifetimes of the

* Corresponding author. Address: Department of Chemistry, 55 North Eagleville Road, University of Connecticut, Storrs, CT 06269-3060, USA. Fax: +1 860 486 6558.
E-mail address: harry.frank@uconn.edu (H.A. Frank).

0009-2614/$ - see front matter © 2010 Elsevier B.V. All rights reserved.
doi:10.1016/j.cplett.2010.05.051

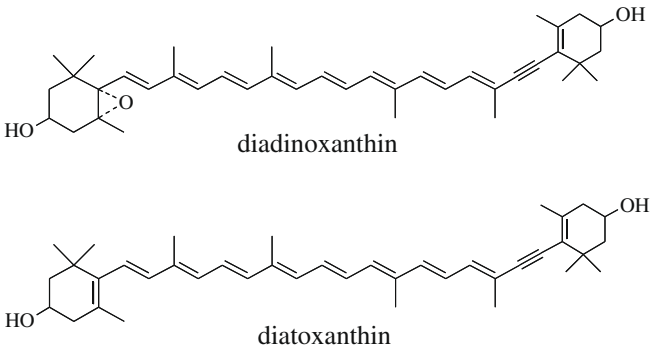

Fig. 1. Molecular structures of diadinoxanthin and diatoxanthin.

molecules and fitting the data to the energy gap law for radiationless transitions [32] which expresses the rate constant for nonradiative deactivation as a function of the energy of the excited state. The values were obtained from a correlation curve constructed from a fit of the energy gap law to S_1 lifetime data obtained from several short chain length carotenoids whose S_1 energies were known from fluorescence studies [20]. Since that time, it has become clear that there exists a systematic error in the S_1 energies obtained by fluorescence and rR spectroscopy due to the fact that these techniques selectively detect the energies of carotenoids whose conformations deviate from idealized C_{2h} symmetry [33,34]. This is because distortions of the molecules induce allowedness into otherwise strongly-forbidden S_1 $(2^1A_g^-) \rightarrow S_0$ $(1^1A_g^-)$ fluorescence and rR spectral bands. A more direct experimental approach that reveals the S_1 energies of undistorted all-trans configurations would be highly desirable for establishing correlations between the photophysics of these molecules and how they function in light harvesting and photoprotection in native organisms. This can be achieved by applying ultrafast transient absorption spectroscopy in the near-infrared (NIR) spectral region to measure the energy of the strongly-allowed S_1 $(2^1A_g^-) \rightarrow S_2$ $(1^1B_u^+)$ transition, and then subtracting this energy from that of the well-resolved and also strongly-allowed, steady-state S_0 $(1^1A_g^-) \rightarrow S_2$ $(1^1B_u^+)$ transition observed in the visible region. In this Letter we report the S_1 energies of diadinoxanthin and diatoxanthin determined in this manner, which has been demonstrated previously to yield highly precise values of the S_1 energies of xanthophylls [33,35–37].

2. Materials and methods

2.1. Sample preparation

Diadinoxanthin and diatoxanthin were obtained from a culture of *P. tricornutum* grown as previously described [38]. In order to stimulate the enzymatic conversion of diadinoxanthin to diatoxanthin, aliquots of *P. tricornutum* culture in the log growth phase were transferred into shallow glass dishes and placed into a growth chamber which was maintained at a constant temperature of 35 °C. The culture was then illuminated using a Cary Model 1471200 tungsten–halogen light source, supplemented with a Reptisun 10.0% UVB 15 W bulb, for 6 h. The xanthophylls were extracted from the whole cells by adding acetone/methanol (1/1, v/v) and centrifuging the mixture at 3000*g* for 5 min. The supernatant containing the pigments was collected and dried in the dark under a gentle stream of nitrogen gas. The dried pigments were then dissolved in acetonitrile and injected into a Millipore Waters 600E HPLC system equipped with a diode array detector and employing a Nova-Pak C_{18} column (300×3.9 mm with 4 μm particle size). The mobile phase, consisting of A = acetonitrile/methanol/water (87/10/3, v/v/v) and B = ethyl acetate, was programmed as follows: 0–20 min, linear gradient from 90% A and 10% B to 60% A and 40% B; 20–30 min, isocratic 60% A and 40% B. The flow rate was 1.0 mL/min. Upon elution, diadinoxanthin and diatoxanthin were collected separately in small vials and dried with a gentle stream of gaseous nitrogen. The molecules were then re-purified by dissolving in acetonitrile and injecting the separate solutions one at a time into the HPLC with the same column and mobile phase protocol described above. The samples were collected, dried, and stored at −80 °C until ready for use in the spectroscopic measurements.

2.2. Spectroscopic methods

2.2.1. Steady-state and transient absorption spectroscopy

Steady-state absorption spectroscopy was carried out using a Varian Cary 50 UV/Vis spectrophotometer on diadinoxanthin and diatoxanthin in acetone or *n*-hexane at 293 K. Transient absorption spectra were recorded using a femtosecond laser spectrometer system previously described [39]. The transient experiments were done at 293 K on the molecules dissolved in either acetone or *n*-hexane and adjusted to an optical density of ~0.5 in a 2 mm path length quartz cuvette at the excitation wavelengths of either 487 nm or 490 nm for acetone and 479 nm for *n*-hexane. The pump laser beam had an energy of 1 μJ/pulse and a spot size diameter of 1 mm, corresponding to intensity of $\sim 2.4 \times 10^{14}$ photons·cm^{-2} per pulse. Absorption spectra were recorded before and after each transient absorption measurement to check the integrity of the samples. Surface Xplorer Pro (v.1.1.0.17) software was used for chirp correction of the spectroscopic data and for the determination of the number of principal components via single value decomposition (SVD). ASUfit version 3.0 software was employed for global fitting analysis in which the quality of fit was checked based on the residuals plot, and chi square value (χ^2).

3. Results and discussion

Absorption spectra of diadinoxanthin and diatoxanthin recorded at 293 K in acetone are shown in Fig. 2. The steady-state absorption spectra of both molecules, which correspond to the strongly-allowed S_0 $(1^1A_g^-) \rightarrow S_2$ $(1^1B_u^+)$ transition, display three prominent vibronic bands associated with totally symmetric C–C and C=C stretching frequencies of ~1200 and ~1600 cm^{-1}. The resolution of the vibronic bands of the two carotenoids is very similar except for the slightly sharper 0–0 vibronic band of diadianoxanthin relative to diatoxanthin. The spectral fine structure is quantified by ratio of the (0–0) to (0–1) band amplitudes measured from a horizontal line drawn through the absorbance minimum between the two peaks. Expressed as a percent, this ratio is denoted %III/II [40] and was determined to be 56% for diadinoxanthin

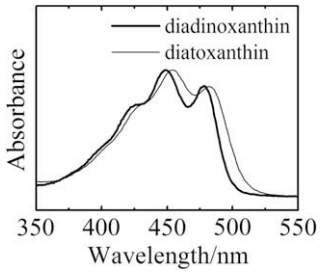

Fig. 2. Steady-state absorption spectra of diadinoxanthin and diatoxanthin in acetone at 293 K. The spectra were normalized to their absorption maxima.

and 34% for diatoxanthin. The difference in the values is due to the epoxide functional group in diadinoxanthin which imposes less conformational disorder on the polyene chain compared to the de-epoxidized diatoxanthin, which possesses a more flexible terminal β-ring [41]. Also, the absorption spectrum of diatoxanthin is red-shifted by ~5 nm relative to diadinoxanthin due to the fact that diatoxanthin has one extra carbon–carbon double bond in its conjugated π-electron system (Fig. 1) which lowers the energy of the $S_0 \rightarrow S_2$ transition.

Transient absorption spectra of diadinoxanthin and diatoxanthin recorded at 293 K in acetone in the visible and NIR regions after excitation into the 0–0 bands of their $S_0 \rightarrow S_2$ transitions are shown in Fig. 3. In the visible region (Fig. 3A and B) after photoexcitation, there is an immediate onset of a bleaching of the ground state absorption band accompanied by the buildup of an $S_1 \rightarrow S_N$ transient absorption band that becomes more intense as time progresses from 0 to 1 ps. Also seen in the visible region is the fact that the $S_1 \rightarrow S_N$ transient absorption spectrum of diatoxanthin is red-shifted by ~36 nm and broader compared to the spectrum of diadinoxanthin. As mentioned above for the steady-state spectra, the spectral red-shift is a result of the increase in the number of conjugated carbon–carbon double bonds in going from diadinoxanthin to diatoxanthin. The broadening in the diatoxanthin spectrum occurs due to conformational disorder induced in the extended polyene chain by the presence of the terminal β-ring [41].

In the NIR region the major feature in the transient absorption spectra of the two xanthophylls appears at a very similar position near 1000 nm (Fig. 3C and D), but like the steady-state and transient spectra in the visible region, the transient absorption band of diatoxanthin is slightly broader than that of diadinoxanthin. The intensity of this transient absorption band decreases by nearly an order of magnitude within 400 fs for both xanthophylls. This rapid decrease in amplitude indicates that the spectral feature at 1000 nm corresponds to an $S_2 \rightarrow S_N$ transition. However, additional weaker bands are observed at longer wavelength that persist for longer times, the strongest of which for both molecules appears at around 1240 nm (Fig. 3C and D). These bands correspond to a transition between the S_1 and S_2 states, and as will be shown below, can be used to determine the precise energies of the S_1 states of the molecules.

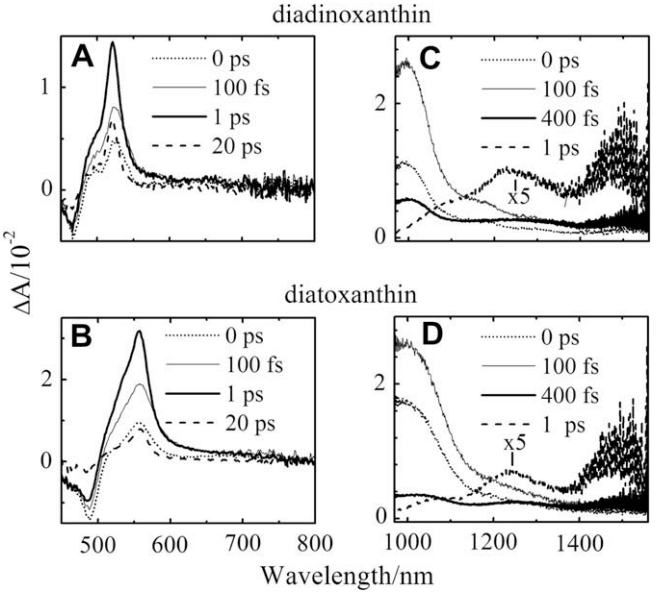

Fig. 3. Transient absorption spectra of diadinoxanthin and diatoxanthin in the visible and NIR regions taken in acetone at 293 K at various time delays after photoexcitation.

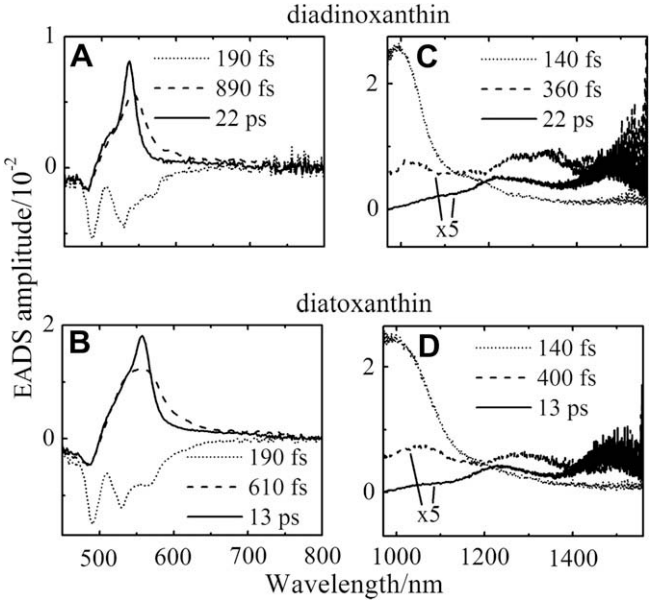

Fig. 4. Global fitting of the transient absorption data shown in Fig. 3 to a sequential (EADS) decay model.

Fig. 4 shows the results of a global analysis of the transient absorption datasets in the visible (Fig. 4A and B) and NIR (Fig. 4C and D) regions fit by a model assuming a sequential decay of the carotenoid excited states formed after photoexcitation into S_2. The lineshapes displayed in Fig. 4 are termed evolution associated difference spectra (EADS). For both molecules in both spectral regions, three kinetic components were needed to obtain an acceptable fit to the data as determined from a consideration of the residual matrix and chi square (χ^2) values.

In the visible region between 460 and 600 nm the first EADS component for both xanthophylls (dotted lines in Fig. 4A and B) decays in 190 fs and shows ground state bleaching and stimulated emission. This first EADS component evolves into a second EADS component (dashed lines in Fig. 4A and B), containing features associated with $S_1 \rightarrow S_N$ excited state absorption. However, the fast kinetics (890 fs for diadinoxanthin and 610 fs for diatoxanthin) and narrowing of the lineshape accompanying the decay of this feature into the third EADS component (solid lines in Fig. 4A and B) indicate that the second EADS is associated with a transition originating from a vibrationally hot S_1 state [42]. The narrower third EADS (solid lines in Fig. 4A and B) are thus associated with a transition from the vibrationally relaxed S_1 state to S_N. This final EADS component decays in 22 ± 1 ps for diadinoxanthin and 13.0 ± 0.5 ps for diatoxanthin, and these represent the S_1 excited state lifetimes of the molecules in good agreement with previously published measurements of 22.8 ps and 13.3 ps, respectively [20]. The distinction between the S_1 kinetics of the two molecules is evident from kinetic traces shown in Fig. 5 which were recorded at the maxima of the $S_1 \rightarrow S_N$ excited state absorption bands (537 nm for diadinoxanthin and 556 nm for diatoxanthin).

The values of the kinetic components obtained from a global fit to the spectral datasets in the NIR region (Fig. 4C and D) are very similar to those obtained in the visible region (Figs. 4A and B). The values in the NIR were obtained by manually fixing the S_1 lifetimes to those measured precisely and accurately in the visible region and then allowing the two faster kinetic components to float freely. The results show that the first NIR EADS component (Fig. 4C and D) is associated with excited state absorption from S_2

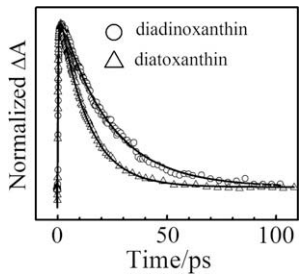

Fig. 5. Kinetic traces recorded at the maxima of the $S_1 \rightarrow S_N$ transient absorption bands. The wavelengths were 537 nm for diadinoxanthin and 556 nm for diatoxanthin. The solid lines correspond to fits obtained from global fitting.

to S_N that decays rapidly into a second EADS component having very low amplitude in this spectral region. The EADS bands at ~1250 nm in this second component become narrower and red-shift as the third EADS component is formed. This is indicative of vibrational cooling in the S_1 state and consistent with that seen in the visible EADS traces (Fig. 4A and B). Moreover, the third EADS traces have spectral bands very similar to those of the steady-state $S_0 \rightarrow S_2$ spectra. This is more clearly seen in Fig. 6 by overlaying the NIR transient absorption bands recorded at a 2 ps time delay with the steady-state $S_0 \rightarrow S_2$ spectra. The strong similarity between the lineshapes indicates that the NIR spectra are associated with $S_1 \rightarrow S_2$ transitions. The values of the S_1 state energies of diadinoxanthin and diatoxanthin were obtained by determining the shift in energy required for the NIR vibronic band positions and spacings to neatly coincide with those of their corresponding visible spectra (Fig. 6). The energy shift is equivalent to the difference between the steady-state $S_0 \rightarrow S_2$ and NIR $S_1 \rightarrow S_2$ transitions and yields the S_1 state energies of the molecules. Fig. 6 shows that precise agreement between the NIR and visible spectra occurs when the S_1 energies are $14\,120 \pm 80\ cm^{-1}$ for diadinoxanthin and $13\,930 \pm 80\ cm^{-1}$ for diatoxanthin. These values are remarkably similar to those reported for two higher plant xanthophylls having an equivalent number of conjugated double bonds, *N*. Lutein ($N = 10$) and zeaxanthin ($N = 11$) have been found to have S_1 energies of $14\,300 \pm 30\ cm^{-1}$ and $13\,950 \pm 30\ cm^{-1}$, respectively [37]. To examine whether there

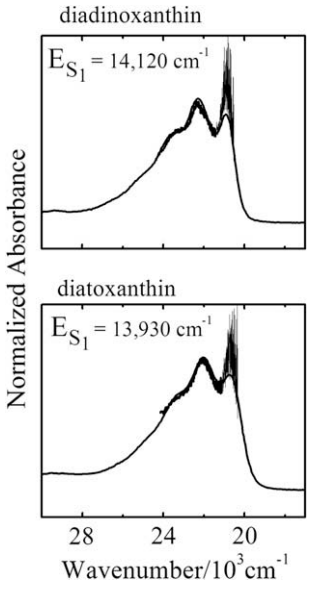

Fig. 6. Overlay of the steady-state $S_0 \rightarrow S_2$ spectra (smooth traces) and the transient $S_1 \rightarrow S_2$ absorption spectra (traces with noise) taken in acetone at 293 K, the latter of which were shifted from the NIR region by the indicated amount of energy. Additional noise observed in the NIR spectral lineshapes below $21\,100\ cm^{-1}$ is due to a weak continuum probe intensity in this spectral region.

was any effect of solvent environment, steady-state and transient spectra were taken not only on the molecules dissolved in acetone, but also in the non-polar solvent, *n*-hexane. The S_1 energies determined in this solvent were $14\,170 \pm 80\ cm^{-1}$ for diadinoxanthin and $13\,980 \pm 80\ cm^{-1}$ for diatoxanthin; i.e. within the range of the uncertainties of the measurements in acetone.

Unlike the previous determination of the S_1 energies of these molecules based on measurements of the S_1 lifetimes of diadinoxanthin and diatoxanthin and an extrapolation from a fit to the energy gap law for radiationless transitions [20], the present data indicate that S_1 energies of both diadinoxanthin and diatoxanthin lie below the S_1 energy of Chl *a* which is $14\,700\ cm^{-1}$ (assuming the Chl *a* Q_y transition occurs at 680 nm). Moreover, the $190\ cm^{-1}$ difference in S_1 energies between diadinoxanthin and diatoxanthin is so small that it would be difficult to understand how diatoxanthin could impart a significant advantage over diadinoxanthin for photoprotection via direct energy transfer from the S_1 state of Chl *a* to the S_1 state of the xanthophyll. Alternatively, the structural modification brought about by de-epoxidizing diadinoxanthin to diatoxanthin during high light stress may trigger either a conformational change in the light-harvesting complex in which these molecules are bound or a change in the nature of the aggregation state of the antenna in order to generate excited state quenching for the protection of the organism. Experiments aimed at evaluating these possibilities are underway.

Acknowledgement

This work has been supported in the laboratory of HAF by a grant from the National Science Foundation (MCB-0913022) and by the University of Connecticut Research Foundation.

References

[1] H.H. Strain, W.M. Manning, G. Hardin, Biol. Bull. 86 (1944) 169.
[2] J.L. Stauber, S.W. Jeffrey, J. Phycol. 24 (1988) 158.
[3] G. Guglielmi, J. Lavaud, B. Rousseau, A.-L. Etienne, J. Houmard, A.V. Ruban, FEBS Lett. 272 (2005) 4339.
[4] J. Lavaud, B. Rousseau, H.J. van Gorkom, A.-L. Etienne, Plant Physiol. 129 (2002) 1398.
[5] A. Hagar, in: F.C. Czygan (Ed.), Pigments in Plants, Fisher, Stuttgart, 1980, p. 57.
[6] H.Y. Yamamoto, Meth. Enzymol. 110 (1985) 303.
[7] S. Demers, S. Roy, R. Gagnon, C. Vignault, Mar. Ecol. Progr. Ser. 76 (1991) 185.
[8] M. Olaizola, J. Laroche, Z. Kolber, P.G. Falkowski, Photosynth. Res. 41 (1994) 357.
[9] B. Demmig-Adams, Biochim. Biophys. Acta 1020 (1990) 1.
[10] H.A. Frank, Arch. Biochem. Biophys. 385 (2001) 53.
[11] A.V. Ruban et al., Nature 450 (2007) 575.
[12] N.E. Holt, D. Zigmantas, L. Valkunas, X.P. Li, K.K. Niyogi, G.R. Fleming, Science 307 (2005) 433.
[13] A.V. Ruban, D. Rees, A.A. Pascal, P. Horton, Biochim. Biophys. Acta 1102 (1992) 39.
[14] C.W. Mullineaux, A.A. Pascal, P. Horton, A.R. Holzwarth, Biochim. Biophys. Acta 1141 (1993) 23.
[15] P. Horton, A. Ruban, J. Exp. Bot. 56 (2005) 365.
[16] R. Pariser, J. Chem. Phys. 24 (1955) 250.
[17] P.R. Callis, T.W. Scott, A.C. Albrecht, J. Chem. Phys. 78 (1983) 16.
[18] R.R. Birge, Acc. Chem. Res. 19 (1986) 138.
[19] V. Chynwat, H.A. Frank, Chem. Phys. 194 (1995) 237.
[20] H.A. Frank, A. Cua, V. Chynwat, A. Young, D. Gosztola, M.R. Wasielewski, Biochim. Biophys. Acta 1277 (1996) 243.
[21] H.A. Frank et al., J. Phys. Chem. B 106 (2002) 2083.
[22] R. Fujii, K. Onaka, M. Kuki, Y. Koyama, Y. Watanabe, Chem. Phys. Lett. 288 (1998) 847.
[23] H.A. Frank, J.A. Bautista, J.S. Josue, A.J. Young, Biochemistry 39 (2000) 2831.
[24] R. Fujii et al., J. Phys. Chem. A 105 (2001) 5348.
[25] J.S. Josue, H.A. Frank, J. Phys. Chem. A 106 (2002) 4815.
[26] T. Sashima, H. Nagae, M. Kuki, Y. Koyama, Chem. Phys. Lett. 299 (1999) 187.
[27] T. Sashima, Y. Koyama, T. Yamada, H. Hashimoto, J. Phys. Chem. B 104 (2000) 5011.
[28] K. Furuichi, T. Sashima, Y. Koyama, Chem. Phys. Lett. 356 (2002) 547.
[29] P.J. Walla, J. Yom, B.P. Krueger, G.R. Fleming, J. Phys. Chem. B 104 (2000) 4799.
[30] P.J. Walla, P.A. Linden, K. Ohta, G.R. Fleming, J. Phys. Chem. A 106 (2002) 1909.
[31] S. Shima et al., J. Phys. Chem. A 107 (2003) 8052.
[32] R. Englman, J. Jortner, Mol. Phys. 18 (1970) 145.

[33] T. Polívka et al., J. Phys. Chem. B 105 (2001) 1072.
[34] T. Polívka, V. Sundström, Chem. Rev. 104 (2004) 2021.
[35] T. Polívka, J.L. Herek, D. Zigmantas, H.E. Akerlund, V. Sundström, Proc. Nat. Acad. Sci. USA 96 (1999) 4914.
[36] D.M. Niedzwiedzki et al., Chem. Phys. 357 (2009) 4.
[37] D.M. Niedzwiedzki, M.M. Enriquez, A.M. LaFountain, H.A. Frank, Chem. Phys. (2010), doi:10.1016/j.chemphys.2010.01.019.
[38] R.R. Guillard, J.H. Ryther, Can. J. Microbiol. 8 (1962) 229.
[39] R.P. Ilagan et al., Biochemistry 45 (2006) 14052.
[40] G. Britton, S. Liaaen-Jensen, H. Pfander (Eds.), Spectroscopy, Birkhauser, Boston, 1995.
[41] R.L. Christensen, B.E. Kohler, Photochem. Photobiol. 18 (1973) 293.
[42] D.M. Niedzwiedzki, J.O. Sullivan, T. Polivka, R.R. Birge, H.A. Frank, J. Phys. Chem. B 110 (2006) 22872.